1521-009X/12/4011-2174–2184$25.00
DRUG METABOLISM AND DISPOSITION
DMD 40:2174–2184, 2012

Vol. 40, No. 11
47530/3802421

Cytochrome P450-Mediated Oxidative Metabolism of Abused Synthetic Cannabinoids Found in K2/Spice: Identification of Novel Cannabinoid Receptor Ligands[S]

Krishna C. Chimalakonda, Kathryn A. Seely, Stacie M. Bratton, Lisa K. Brents, Cindy L. Moran, Gregory W. Endres, Laura P. James, Paul F. Hollenberg, Paul L. Prather, Anna Radominska-Pandya, and Jeffery H. Moran

Departments of Pharmacology and Toxicology (K.C.C., L.K.B., L.P.J., P.L.P., J.H.M.) and Biochemistry and Molecular Biology (S.M.B., A.R.-P.), College of Medicine, University of Arkansas for Medical Sciences, Little Rock, Arkansas; Arkansas Department of Health, Arkansas Public Health Laboratory, Little Rock, Arkansas (K.A.S., J.H.M.); Arkansas State Crime Laboratory, Little Rock, Arkansas (C.L.M.); Clinical Pharmacology and Toxicology, Arkansas Children's Hospital and Department of Pediatrics, College of Medicine, University of Arkansas for Medical Sciences, Little Rock, Arkansas (L.P.J.); Cayman Chemical Company, Ann Arbor, Michigan (G.W.E.); and Department of Pharmacology, University of Michigan Medical School, Ann Arbor, Michigan (P.F.H.)

Received June 28, 2012; accepted August 17, 2012

ABSTRACT:

Abuse of synthetic cannabinoids (SCs), such as [1-naphthalenyl-(1-pentyl-1*H*-indol-3-yl]-methanone (JWH-018) and [1-(5-fluoropentyl)-1*H*-indol-3-yl]-1-naphthalenyl-methanone (AM2201), is increasing at an alarming rate. Although very little is known about the metabolism and toxicology of these popular designer drugs, mass spectrometric analysis of human urine specimens after JWH-018 and AM2201 exposure identified monohydroxylated and carboxylated derivatives as major metabolites. The present study extends these initial findings by testing the hypothesis that JWH-018 and its fluorinated counterpart AM2201 are subject to cytochrome P450 (P450)-mediated oxidation, forming potent hydroxylated metabolites that retain significant affinity and activity at the cannabinoid 1 (CB_1) receptor. Kinetic analysis using human liver microsomes and recombinant human protein identified CYP2C9 and CYP1A2 as major P450s involved in the oxidation of the JWH-018 and AM2201. In vitro metabolite formation mirrored human urinary metabolic profiles, and each of the primary enzymes exhibited high affinity (K_m = 0.81–7.3 μM) and low to high reaction velocities (V_{max} = 0.0053–2.7 nmol of product · min^{-1} · nmol $protein^{-1}$). The contribution of CYP2C19, 2D6, 2E1, and 3A4 in the hepatic metabolic clearance of these synthetic cannabinoids was minimal (f_m = <0.2). In vitro studies demonstrated that the primary metabolites produced in humans display high affinity and intrinsic activity at the CB_1 receptor, which was attenuated by the CB_1 receptor antagonist (6*aR*,10*aR*)-3-(1-methanesulfonylamino-4-hexyn-6-yl)-6*a*,7,10,10*a*-tetrahydro-6,6,9-trimethyl-6*H*-dibenzo[*b,d*]pyran (O-2050). Results from the present study provide critical, missing data related to potential toxicological properties of "K2" parent compounds and their human metabolites, including mechanism(s) of action at cannabinoid receptors.

This work was funded by the National Institutes of Health National Institute of General Medical Sciences [Grant GM075893] (to A.R.-P.); Association of Public Health Laboratories [Innovation Award] (to J.H.M.); and the University of Arkansas for Medical Sciences Translational Research Institute (to C.L.), which is funded by the National Center for the Advancement of Translational Science [UL1-TR000039].

Article, publication date, and citation information can be found at http://dmd.aspetjournals.org.

http://dx.doi.org/10.1124/dmd.112.047530.

[S] The online version of this article (available at http://dmd.aspetjournals.org) contains supplemental material.

Introduction

Although cannabis (also called marijuana) remains one of the most abused drugs in the United States (Banken, 2004; Seely et al., 2011, 2012), synthetic cannabinoids are gaining popularity among recreational drug users as adulterants of herbal products commonly marketed as "K2" or "Spice" (Kudo et al., 1995; European Monitoring Centre for Drugs and Drug Addiction, 2009; Atwood et al., 2010; Dresen et al., 2010; Seely et al., 2011, 2012). [1-naphthalenyl-(1-pentyl-1*H*-indol-3-yl]-methanone (JWH-018) and [1-(5-fluoropentyl)-1*H*-indol-3-yl]-1-naphthalenyl-methanone (AM2201) represent

ABBREVIATIONS: JWH-018, [1-naphthalenyl-(1-pentyl-1*H*-indol-3-yl]-methanone; AM2201, [1-(5-fluoropentyl)-1*H*-indol-3-yl]-1-naphthalenyl-methanone; CB_1, cannabinoid type 1 receptor; CB_2, cannabinoid type 2 receptor; P450, cytochrome P450; HLM, human liver microsomes; CP-55,940, 5-(1,1-dimethylheptyl)-2-(5-hydroxy-2-(3-hydroxypropyl)cyclohexyl)phenol; O-2050, (6*aR*,10*aR*)-3-(1-methanesulfonylamino-4-hexyn-6-yl)-6*a*,7,10,10*a*-tetrahydro-6,6,9-trimethyl-6*H*-dibenzo[*b,d*]pyran; GTPγS, guanosine 5′-*O*-(3-thio)triphosphate; OR, oxidoreductase; MS/MS, tandem mass spectrometry; SRM, specific reaction monitoring; IDA, information-dependent acquisition; EPI, enhanced product ion; BSA, bovine serum albumin; WIN55,212-2, (*R*)-(+)-[2,3-dihydro-5-methyl-3-(4-morpholinylmethyl) pyrrolo-[1,2,3-*d,e*]-1,4-benzoxazin-6-yl]-1-naphthalenyl-methanone (WIN-55,212-2); ANOVA, analysis of variance.

two common derivatives structurally characterized as aminoalkylindoles (Compton et al., 1992a,b; Atwood et al., 2010). These derivatives were first synthesized in the early 1990s to study the pharmacology of the cannabinoid type 1 (CB_1) receptor, the predominant G-protein-coupled receptor in the brain, and the cannabinoid type 2 (CB_2) receptor, located on immune cells (Huffman and Padgett, 2005; Mackie, 2008). Receptor binding studies have shown JWH-018 (Atwood et al., 2010; Brents et al., 2011) and other aminoalkylindoles to be high-affinity ligands (Ward et al., 1990; Thakur et al., 2005) at CB_1 and CB_2 receptors. Synthetic cannabinoids have potential therapeutic benefits because of their antiemetic and pain-relieving properties (Seely et al., 2011); however, most synthetic cannabinoids synthesized to date have not been approved for human use because of toxic side effects and undesirable psychoactive properties (Camp, 2011; Wells and Ott, 2011).

Whereas use of cannabis, which contains the natural psychoactive cannabinoid Δ^9-tetrahydrocannabinol (Δ^9-THC), is often associated with mild symptoms such as appetite stimulation and orthostatic hypotension (Jones, 2002; Randall et al., 2004), K2 users present to emergency departments with severe adverse effects including hypertension, visual and auditory hallucinations, tachycardia, sinus bradycardia, chest pain, dysrhythmias, seizures, psychosis, intracranial hemorrhage, and even death (Müller et al., 2010; Vearrier and Osterhoudt, 2010; Benford and Caplan, 2011; Every-Palmer, 2011; Lapoint et al., 2011; Schneir et al., 2011; Simmons et al., 2011a,b; Young et al., 2011; Pant et al., 2012). In addition, recent medical reports indicate that chronic K2 use may lead to the development of tolerance, dependence, and withdrawal (Zimmermann et al., 2009), as has been observed with marijuana abuse (Budney and Hughes, 2006).

Little information is known about the metabolism and pharmacology of these emerging drugs of abuse. We and others have identified several hydroxylated metabolites of JWH-018 and AM2201 in humans with a known history of K2 use, implicating the role of mixed-function oxidases, such as cytochromes P450, in the biotransformation of synthetic cannabinoids (Zhang et al., 2002; Sobolevsky et al., 2010; Wintermeyer et al., 2010; Chimalakonda et al., 2011b; Moran et al., 2011; Hutter et al., 2012). Previous reports showed that JWH-018 undergoes hepatic metabolism, leading to the formation of several naphthalene, indole, and alkyl side chain hydroxylated and carboxylated metabolites (Fig. 1), which are subsequently conjugated by UDP-glucuronosyltransferases and excreted as glucuronic acid conjugates in human urine (Chimalakonda et al., 2011a,b). In addition, a recent study by Brents et al. (2011) demonstrated that the ring and side chain hydroxylated derivatives of JWH-018 possessed greater in vitro and in vivo pharmacological activity than Δ^9-THC, indicating that oxidative biotransformation does not terminate the pharmacological activity of JWH-018. Thus, compared with Δ^9-THC, the increased severity and frequency of adverse effects of K2 may be explained, in part, by the generation of biologically active metabolites that may prolong or intensify CB_1 receptor activation. This important observation exemplifies the necessity for characterizing the specific metabolic pathways responsible for the biotransformation of these new, emerging drugs of abuse.

The purpose of this study was to identify specific P450 isoforms responsible for JWH-018 and AM2201 oxidation and to determine whether primary human *ω*-(1-(5-hydroxypentyl)-1*H*-indol-3-yl)(naphthalen-1-yl)-methanone) and *ω*-1-hydroxylated (1-(4-hydroxypentyl)-1*H*-indol-3-yl)(naphthalen-1-yl)methanone) and (1-(5-fluoro-4-hydroxypentyl)-1*H*-indol-3-yl)(naphthalen-1-yl)methanone) metabolites

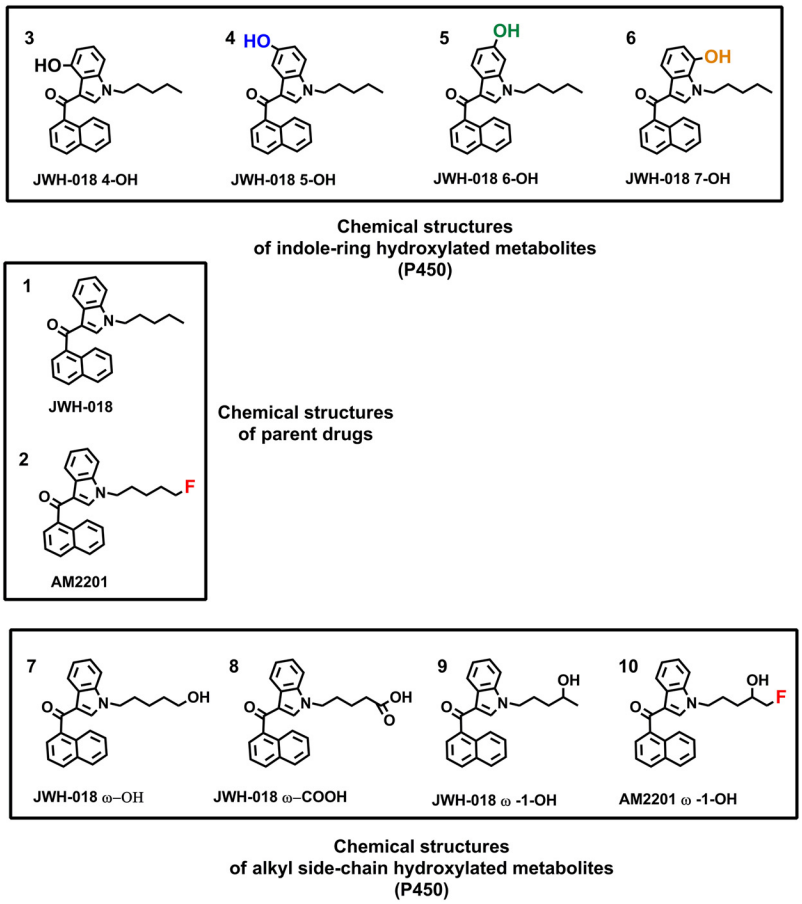

FIG. 1. Structures of JWH-018 and AM2201 and hydroxyl metabolites. JWH-018 (**1**) and AM2201 (**2**) are structurally similar, with AM2201 differing by the presence of terminal alkyl fluorine atom. The ring hydroxylated metabolites shown are JWH-018 4-OH (**3**), JWH-018 5-OH (**4**), JWH-018 6-OH (**5**), and JWH-018 7-OH (**6**) and alkyl side chain metabolites are JWH-018 *ω*-OH (**7**), JWH-018 *ω*-COOH (**8**), JWH-018 *ω*-1-OH (**9**), and AM2201 *ω*-1-OH (**10**).

of JWH-018 and AM2201 bind to and activate CB_1 receptors. Data reported herein indicate that CYP2C9 and CYP1A2 are the major human isoforms involved in the oxidation of JWH-018 and AM2201 and that oxidized metabolites of each compound display nanomolar affinity and intrinsic activity at mouse CB_1 receptors.

Materials and Methods

Materials. All chemicals used for this study were of reagent grade or higher. Analytical standards for JWH-018, AM2201, and their hydroxylated and carboxylated metabolites (Fig. 1) were kindly provided by Cayman Chemical Company (Ann Arbor, MI). cDNA-expressed human recombinant cytochrome P450 enzymes (BD-Supersomes), pooled human liver microsomes (HLM) (50-donor pool), and the NADPH-regenerating system (20 mM $NADP^+$, 60 mM glucose 6-phosphate, 60 mM $MgCl_2$, and 100 U/ml glucose 6-phosphate dehydrogenase) were purchased from BD Gentest (Woburn, MA). Optima LC-mass spectrometry-grade acetonitrile and ethanol were purchased from Thermo Fisher Scientific (Waltham, MA). Reagent-grade formic acid (99% pure) was purchased from Acros Organic (Fairlawn, NJ). Deionized water was purified to 18.2 MΩ-cm resistivity using a PURELAB Ultra laboratory water purification system (ELGA, Woodridge, IL). All other chemicals and reagents, unless otherwise specified, were purchased from Sigma-Aldrich (St. Louis, MO).

For CB_1 receptor binding and activity assays, all drugs, with the exception of ω-1-OH metabolites of JWH-018 and AM2201 were diluted to a concentration of 10^{-2} M with 100% ethanol and stored at −20°C. The ω-1-OH metabolites of JWH-018 and AM2201 were diluted to a concentration of 10^{-2} M with 100% dimethyl sulfoxide and stored at −20°C. Δ^9-THC was supplied by the National Institute on Drug Abuse (Bethesda, MD). 5-(1,1-Dimethylheptyl)-2-(5-hydroxy-2-(3-hydroxypropyl)cyclohexyl)phenol (CP-55,940) and (6*aR*,10*aR*)-3-(1-methanesulfonylamino-4-hexyn-6-yl)-6*a*,7,10,10*a*-tetrahydro-6,6,9-trimethyl-6*H*-dibenzo[*b*,*d*]pyran (O-2050) were purchased from Tocris Bioscience (Ellisville, MO). GTPγS and GDP were purchased from EMD Chemicals (Gibbstown, NJ) and Sigma-Aldrich, respectively. Both chemicals were diluted to a stock concentration of 10^{-2} M with water and stored at −20°C. [^{3}H]CP-55,940 (174.6 Ci/mmol), used for competition receptor binding, was purchased from PerkinElmer Life and Analytical Sciences (Waltham, MA), and [^{35}S]GTPγS (1250 Ci/mmol) was purchased from American Radiolabeled Chemicals (St. Louis, MO).

Equipment. Kinetic analysis was performed using an API-4000 Q TRAP tandem mass spectrometer (AB SCIEX, Framingham, MA) interfaced with an Series 1200 quaternary liquid chromatography system (Agilent Technologies, Santa Clara, CA). Analyst software (version 1.5; AB SCIEX) was used to control the overall operation of the high-performance liquid chromatography system and the mass spectrometer. For CB_1 receptor binding and intrinsic activity assays, bound radioactivity was determined by an LS6500 liquid scintillation spectrophotometer (Beckman Coulter, Brea, CA).

Screening of JWH-018 and AM2201 Using Human Recombinant P450 Isoforms and Pooled Human Liver Microsomes. To examine the metabolism of JWH-018 and AM2201, cDNA-expressed human recombinant cytochrome P450 enzymes (2 pmol, CYP1A2, -2C9, -2C19, -2D6, -2E1, and -3A4; BD Supersomes) and pooled HLM (50 μg) from a 50-donor pool were assayed for activity toward these compounds. Substrates (JWH-018 and AM2201, 10 μM, final concentration) were added in ethanol and allowed to dry at ambient temperature. Protein was added in the presence of 0.1 M KPO_4 (final concentration) buffer, pH 7.4, with an NADPH-regenerating system (solution A: 20 mM $NADP^+$, 60 mM glucose 6-phosphate, and 60 mM $MgCl_2$; solution B: 100 U/ml glucose 6-phosphate dehydrogenase) to ensure sufficient NADPH to enable cytochrome P450-mediated reactions. Controls omitting the substrate, protein, and NADPH were included with each assay. To determine whether oxidoreductase (OR) and cytochrome b_5 metabolize JWH-018 and AM2201, a 10 μM final concentration of each was incubated in presence of OR and cytochrome b_5 (50 μg) under similar assay conditions. The total reaction volume was 50 μl, and all incubations were performed in triplicate. Reactions were initiated by the addition of the NADPH-regenerating system, incubated at 37°C for 90 min, and terminated by addition of an equal volume of ethanol. Before LC-MS/MS analysis, protein and other particulates were precipitated by centrifugation at 20,800*g* for 5 min.

Steady-State Enzyme Kinetic Assays. For kinetic analysis, incubation conditions were optimized for time and protein concentration. All reactions were performed within the linear range of metabolite formation and less than 5% of substrate was consumed during the course of the reaction (data not shown). Other than substrate concentrations and incubation times, reaction mixture compositions and analytical methods were identical to those described for screening assays above. Kinetic parameters were determined by incubating recombinant CYP1A2, CYP2C9, CYP2C19 (2 pmol each), and CYP2D6 (4 pmol) in the presence of various concentrations of substrate (JWH-018 and AM2201, 0.05–100 μM) for 10 min at 37°C for CYP1A2, CYP2C9, and CYP2C19 and 20 min at 37°C for CYP2D6. For reactions using HLM, various concentrations of substrates (JWH-018 and AM2201, 0.05–100 μM) were incubated with 75 μg of HLM protein for 20 min at 37°C.

LC-MS/MS Analysis. Quantification of analytes of interest was performed using positive ion electrospray ionization LC-MS/MS methods developed previously for trace analysis of synthetic cannabinoid metabolites (Chimalakonda et al., 2011b; Moran et al., 2011). For these studies, analytical standards (0.20–100 ng/ml) were matrix-matched in pooled human urine void of synthetic cannabinoid contamination or in the final in vitro reaction mixture (ethanol-water-0.1 M phosphate buffer, pH 7.4, 50:30:20%). Analytes of interest were chromatographically separated as described previously under isocratic conditions using an Zorbax Eclipse XDB-C18 analytical column (150 × 4.6 mm, 5 μm; Agilent Technologies) heated to 40°C. Mobile phases consisted of 45% A (0.1% formic acid in water) and 55% B (0.1% formic acid in acetonitrile (Chimalakonda et al., 2011b; Moran et al., 2011). The XDB-C18 analytical column was washed and reequilibrated between each injection by ramping mobile phase B to 95% and then returning the system to initial conditions. The TurboIonSpray source voltage was 2500 V, and source temperature was maintained at 600°C. Nitrogen gas pressures for the GS1 and GS2 source gases, curtain gas, and collision gases were 55.0 cm/s, 55.0 cm/s, 35.0 cm/s, and "high," respectively.

Confirmation of each metabolite was determined by including specific reaction monitoring (SRM)-information-dependent acquisitions (IDAs) to obtain enhanced product ion (EPI) spectra for each product. Molecule-specific parameters for SRM-IDA experiments are listed in Supplemental Table 1. The SRM-IDA transition threshold that triggered EPI experiments was fixed at 500 cps. Resulting EPI mass spectra for quality control and unknown specimens were library-matched against stored EPI mass spectra as reported previously (Chimalakonda et al., 2011b; Moran et al., 2011) or obtained from newly synthesized analytical standards to ensure that similar urinary metabolites that may interfere with analysis were fully resolved. Supplemental Figure 1 shows the mass spectra used to confirm the presence of the ω-1-OH metabolite of AM2201 in each reaction and identifies the appropriate molecular ion ([MH^+], *m*/*z* 376) and expected product ions characteristic of aminoalkylindoles (*m*/*z* 127 and 155). In addition to mass spectra comparisons, all metabolic products were confirmed by matching retention times of analytical standards. LC-MS/MS conditions have previously been shown to resolve each of the metabolites assayed from their corresponding conjugates (Chimalakonda et al., 2011a).

β-Glucuronidase Treatment of Subject Samples. To evaluate human urinary metabolic profiles, 40 μl of human urine were incubated in the presence and absence of β-glucuronidase (bovine liver, type B-10; Sigma-Aldrich) at 37°C, with constant shaking for 60 min, by adding 160 μl of 0.1 M sodium acetate buffer, pH 5.0, containing β-glucuronidase (1.6 U/μl final concentration). After incubations, 100 μl of the final reaction mixture was spiked with deuterium-labeled internal standards available for ω-OH and ω-COOH metabolites (100 ng/ml final concentrations) before LC-MS/MS analysis.

Kinetic Data Analysis. Curve-fitting and statistical analyses were conducted using GraphPad Prism (version 4.0b; GraphPad Software Inc., San Diego, CA). Kinetic constants were obtained by fitting experimental data to kinetic models using the nonlinear regression (Curve Fit) function.

The fit of the data for each model was assessed from the S.E., 95% confidence intervals, and R^2 values. Kinetic curves were also analyzed as Eadie-Hofstee plots to support kinetic models. Kinetic constants are reported as the mean ± S.E. of triplicate experiments.

CB_1 Receptor Affinity and Intrinsic Activity Assays: Membrane Preparation. Whole brains were harvested from B6SJL mice, snap-frozen in liquid

nitrogen, and stored at −80°C. B6SJL mice were chosen as a model system because the sequence similarity between mice and human CB_1 receptor is >85%, and B6SJL mice have been used extensively by our laboratory to study CB_1 receptor-mediated pharmacology of various cannabinoids (Brents et al., 2011, 2012). Crude membrane homogenates were prepared on the basis of established methods (Prather et al., 2000). Brains were thawed on ice, pooled, and suspended in ice-cold homogenization buffer (50 mM HEPES, pH 7.4, 3 mM $MgCl_2$, and 1 mM EGTA). Suspended brains were then subjected to 10 complete strokes using a 40-ml Dounce glass homogenizer and centrifuged at 40,000*g* for 10 min at 4°C. Supernatants were discarded, and pellets were resuspended in ice-cold homogenization buffer, homogenized, and centrifuged similarly two more times. After the final centrifugation step, pellets were resuspended in ice-cold 50 mM HEPES, pH 7.4, to a concentration of approximately 2 mg/ml and aliquoted for storage at −80°C. Protein concentration was determined using BCA Protein Assay (Thermo Fisher Scientific).

CB_1 Receptor Binding: Competition Binding Assay. Mouse brain membrane homogenates (50 μg, containing a relatively pure source of CB_1 receptors) were incubated with a 0.2 nM concentration of the radiolabeled cannabinoid agonist [^{3}H]CP-55,940 for 90 min at room temperature in an assay buffer containing 5 mM $MgCl_2$, 50 mM Tris, 0.05% bovine serum albumin (BSA), and increasing concentrations (0.1 nM–10 μM) of JWH-018, AM2201, and their ω-OH (terminal position on the pentyl side chain) and ω-1-OH and ω-COOH (5-(3-(1-naphthoyl)-1*H*-indol-1-yl)-pentanoic acid) metabolites (Fig. 1). Assays were performed in triplicate, in a final volume of 1.0 ml, as described previously (Shoemaker et al., 2005). Total binding was defined as the amount of radioactivity observed when 0.2 nM [^{3}H]CP-55,940 was incubated in the absence of any competitor. Nonspecific binding was defined as the amount of [^{3}H]CP-55,940 binding remaining in the presence of 10 μM concentrations of the nonradioactive and nonselective CB_1/CB_2 receptor agonist (*R*)-(+)-[2,3-dihydro-5-methyl-3-(4-morpholinylmethyl) pyrrolo-[1,2,3-*d*,*e*]-1,4-benzoxazin-6-yl]-1-naphthalenyl-methanone (WIN-55,212-2). Specific binding was calculated by subtracting nonspecific from total binding. Reactions were terminated by quick filtration through Whatman GF/B glass fiber filters, followed by five washes with an ice-cold buffer containing 50 mM Tris and 0.05% BSA. Filters were punched out into 7-ml scintillation vials and immersed in 4 ml of ScintiVerse BD Cocktail scintillation fluid. After overnight extraction, bound radioactivity was determined by liquid scintillation spectrophotometry. Specific binding is expressed as a percentage of binding occurring in vehicle samples (binding in the absence of any competitor).

CB_1 Receptor Functional Assay: [^{35}S]GTPγS Binding. [^{35}S]GTPγS binding was performed as described previously with minor modifications (Prather et al., 2000). Each synthetic cannabinoid or metabolite was incubated with 25 μg of mouse brain membrane homogenates, 10 mM GDP, 0.1 nM [^{35}S]GTPγS, and assay buffer (20 mM HEPES, 10 mM $MgCl_2$, 100 mM NaCl, 20 U/l adenosine deaminase, and 0.05% BSA). Assays were performed in triplicate in a final volume of 1 ml for 30 min at 30°C. Total binding was defined as the amount of radioactivity observed when 0.1 nM [^{35}S]GTPγS was incubated in the absence of any cannabinoid. Nonspecific binding was defined as the amount of [^{35}S]GTPγS binding remaining in the presence of 10 μM nonradioactive GTPγS. Specific binding was calculated by subtracting nonspecific from total binding. Reactions were terminated by quick filtration through Whatman GF/B glass fiber filters, followed by five washes with an ice-cold buffer containing 20 mM HEPES and 0.05% BSA. Filters were punched out into 7-ml scintillation vials and immersed in 4 ml of ScintiVerse BD Cocktail scintillation fluid. After overnight extraction, bound radioactivity was determined by liquid scintillation spectrophotometry. The amount of specific [^{35}S]GTPγS binding produced by each drug was normalized by expressing the G-protein activation for each compound as a percentage of binding produced by the full CB receptor agonist CP-55,940.

Statistical Analysis. Curve fitting and statistical analyses for competition binding experiments were performed using GraphPad Prism. The Cheng-Prusoff (Cheng and Prusoff, 1973) equation was used to convert the experimental IC_{50} values obtained from competition receptor binding experiments to K_i values, a quantitative measure of receptor affinity. Nonlinear regression for one-site competition was used to determine the IC_{50} for competition receptor binding. E_{max} (a measure of efficacy) was calculated as the percentage of specific [^{35}S]GTPγS binding produced by each drug, relative to that produced by the full CB receptor agonist CP-55,940. Data are expressed as means ± S.E.M. A one-way ANOVA, followed by a Newman-Keuls multiple comparison post hoc test, was used to determine statistical significance ($P < 0.05$) between the groups. All statistical calculations were performed using GraphPad Prism.

Results

To begin assessing the physiological relevance of HLM reactions, metabolites produced in vitro were qualitatively compared with metabolic products excreted in human urine collected from individuals suspected of using JWH-018 or AM2201 (Fig. 2). Consistent with

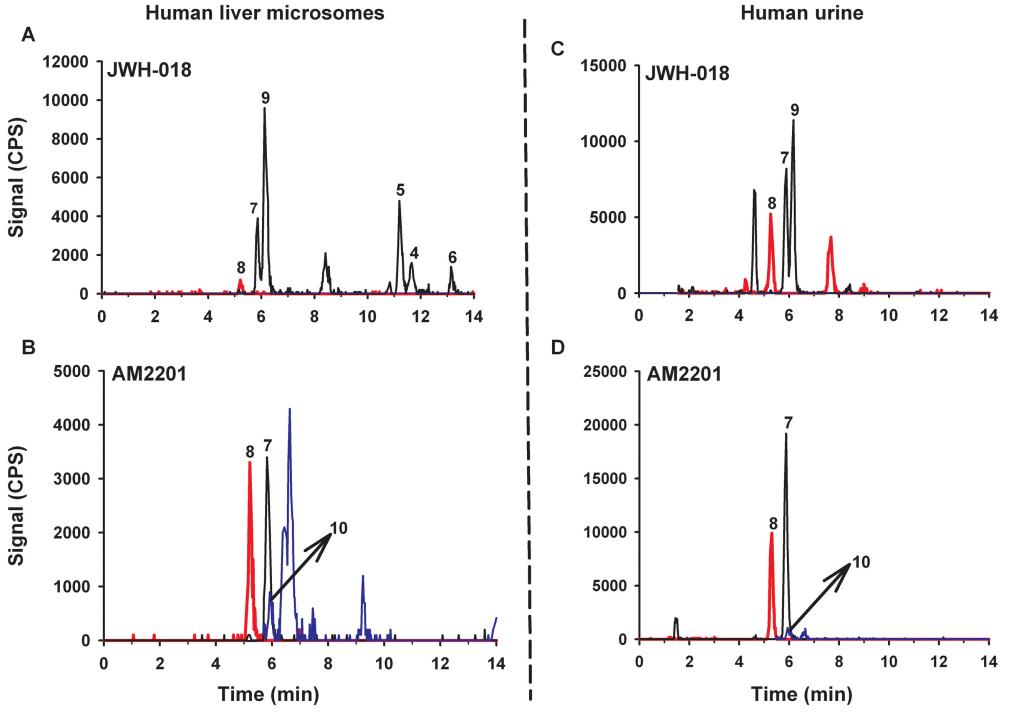

FIG. 2. LC chromatograms of the hydroxyl and carboxyl metabolites of JWH-018 and AM2201 in human liver microsomes and human urine. Resulting chromatographs produced from incubation of 10 μM JWH-018 (A) and AM2201 (B) with 75 μg of HLM as explained under *Materials* and *Methods* and from representative human urine collected after suspected use of JWH-018 (C) or AM2201 (D) are shown. Chromatographs shown were generated after treatment of the urine with β-glucuronidase as described under *Materials and Methods*. The numbers above the chromatographic peaks correspond to the hydroxylated and carboxylated metabolites of JWH-018 and AM2201 shown in Fig. 1. Concentrations of the respective metabolites in B are as follows: JWH-018 ω-OH (8.53 ng/ml), JWH-018 ω-COOH (4.7 ng/ml), and JWH-018 ω-1-OH (9.6 ng/ml). Concentrations of respective metabolites in D are as follows: JWH-018 ω-OH (19.6 ng/ml), JWH-018 ω-COOH (9.2 ng/ml), and JWH-018 ω-1-OH (1.06 ng/ml). Different color tracings are representative of the SRM experiments (Supplemental Table 1) used to detect analytes **1** to **10** (Fig. 1). Specific LC-MS/MS conditions are provided under *Materials and Methods*.

previous reports, JWH-018 and AM2201 appear to be metabolized similarly to produce several ring and alkyl side chain oxidized metabolites that are excreted in human urine as glucuronic acid conjugates (Chimalakonda et al., 2011b; Moran et al., 2011). It also appears that AM2201 readily undergoes cytochrome P450-mediated oxidative dehalogenation to produce common metabolites with JWH-018, whereas the ω-1-OH metabolites of each synthetic cannabinoid are distinct. In vitro reactions led to the formation of three different indole ring-substituted oxidized metabolites (Fig. 2), but these metabolites were not detected in the human specimens. The physiological significance of this finding remains to be determined. Although it is difficult to extrapolate urinary concentrations to toxicological endpoints, data identify the pentyl alkyl side chain present in both JWH-018 and AM2201 (Fig. 1) as the primary site for P450-mediated oxidation in humans.

To further assess metabolic pathways responsible for JWH-018 and AM2201 oxidation, six human recombinant P450 isoforms listed in Fig. 3 were screened for their ability to mediate JWH-018 and AM2201 oxidation. All screening assays used a 10 μM substrate concentration to maximize the potential for identifying all oxidized products. Reaction velocities were estimated by determining the concentration of the ω-OH, ω-COOH, ω-1-OH, and indole ring-oxidized metabolites (Fig. 1) using established LC-MS/MS methods, previously validated for trace level quantification (Chimalakonda et al., 2011b; Moran et al., 2011). After normalizing reaction velocities to hepatic abundance (Rowland-Yeo et al., 2003), CYP1A2 and CYP2C9 exhibited the most activity toward JWH-018 and AM2201 oxidation, whereas much less contribution from CYP2C19, 2D6, 2E1, and 3A4 was observed (Fig. 3). No interfering products were identified in negative control reactions omitting either substrates or cofactor (data not shown). Incubation of JWH-018 with OR and cytochrome b_5 led to the formation of the JWH-018 5-OH metabolite (5-hydroxy-1-pentyl-1*H*-indol-3-yl)(naphthalen-1-yl)methanone (~12 nM, data not shown). The concentration of unidentified-OH metabolites of JWH-018 and AM2201 reported in Supplemental Tables 2 to 5 was estimated from standard responses obtained using the JWH-018 ω-OH analytical standard.

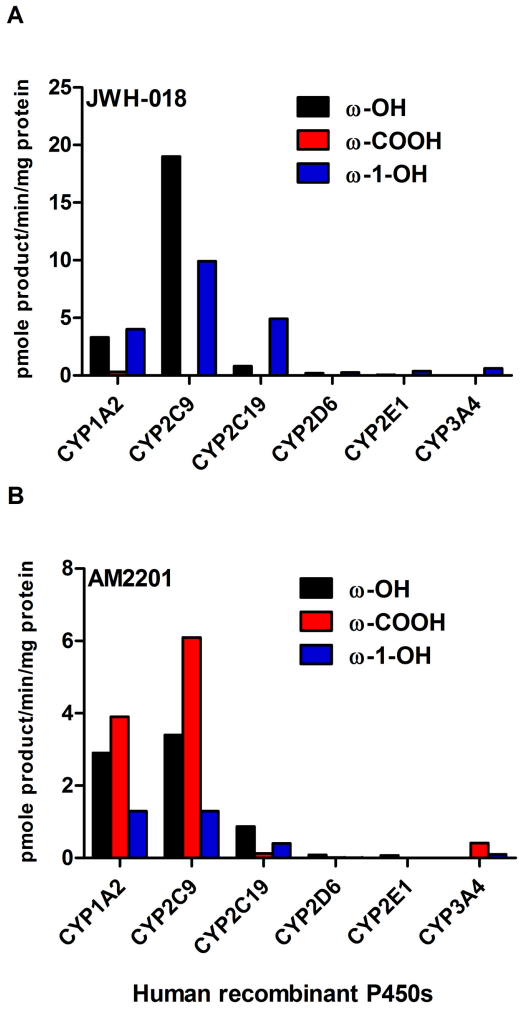

FIG. 3. Oxidation of JWH-018 (A) and AM2201 (B) by human recombinant cytochromes P450. Oxidation of JWH-018 (A) and AM2201 (B) to ω-OH, ω-1-OH, and ω-COOH metabolites. Activity is normalized to hepatic abundance of specific P450s (Rowland-Yeo et al., 2003) and is expressed as picomoles of product per minute per milligram protein.

Oxidized products produced during reactions with each recombinant protein (Fig. 4) were also qualitatively compared with metabolic profiles observed in human specimens (Fig. 2). Similar to metabolic profiles observed in human urine specimens, CYP1A2 reactions with JWH-018 produced the ω-OH, ω-COOH, and ω-1-OH metabolites along with a single indole ring-oxidized metabolite (Fig. 4A). Of interest, CYP1A2 is the only isoform that produced the ω-COOH derivative in the presence of JWH-018. CYP2C9 produced equivalent levels of the ω-OH and ω-1-OH metabolites (Fig. 4B), whereas CPY2C19 predominantly catalyzed the formation of the ω-1-OH metabolite (Fig. 4C). CYP2D6 catalyzes the formation of several indole ring-oxidized derivatives along with the formation of the alkyl side chain oxidized metabolites (Fig. 4D).

CYP1A2, CYP2C9, and CYP2C19 all mediated oxidative dehalogenation reactions in the presence of AM2201 to form the ω-OH and the ω-COOH metabolites (Fig. 4, E–G), but, in addition, the ω-1-OH derivative of AM2201 along with an unidentified-OH metabolite was also formed. In general, incubation of AM2201 with CYP2D6 led to overall lower metabolite formation in comparison with CYP1A2, CYP2C9, and CYP2C19, but sufficient activity led to the identification of ω-OH and the unidentified-OH derivatives as major AM2201 metabolites (Fig. 4H).

Kinetic Analysis. Screening data indicate a significant role for CYP2C9 and CYP1A2 in the oxidation of JWH-018 and AM2201. Therefore, the kinetic analysis of JWH-018 and AM2201 oxidation in HLM was compared with that of recombinant CYP2C9 and CYP1A2 to further assess the overall contribution of these enzymes in synthetic cannabinoid metabolism. The formation of ω-OH and ω-1-OH metabolites of JWH-018 in HLM exhibited saturable hyperbolic kinetics consistent with a Michaelis-Menten kinetic profile (Table 1; Supplemental Fig. 3A), whereas the kinetic profile for the formation of indole ring-oxidized (metabolites **3–6**; Fig. 1) and an unidentified-OH derivative of JWH-018 exhibited Michaelis-Menten or Hill activation kinetics, respectively (Supplemental Table 2; Supplemental Fig. 6A).

Kinetic analysis of JWH-018 oxidation with human recombinant CYP1A2 exhibited classic Michaelis-Menten kinetics for the formation of ω-OH and ω-1-OH derivatives, with high affinity (low apparent K_m values ranging from 4.7–5.3 μM) and high capacity (V_{max} = 833-1438 pmol of product · min^{-1} · nmol $protein^{-1}$), whereas the kinetic profile for the formation of the ω-COOH metabolite with CYP1A2 exhibited substrate inhibition (SI). The ω-OH and ω-1-OH metabolite formation with recombinant CYP2C9 exhibited activation kinetics fitting the Hill equation, with high affinity (low apparent K_m = 0.81–1.3 μM) and high capacity (V_{max} = 487–835 pmol of product · min^{-1} · nmol $protein^{-1}$) (Table 1; Supplemental Fig. 4).

HLM reactions with AM2201 followed either classic Michaelis-Menten kinetics or a biphasic kinetic profile (Table 2; Supplemental

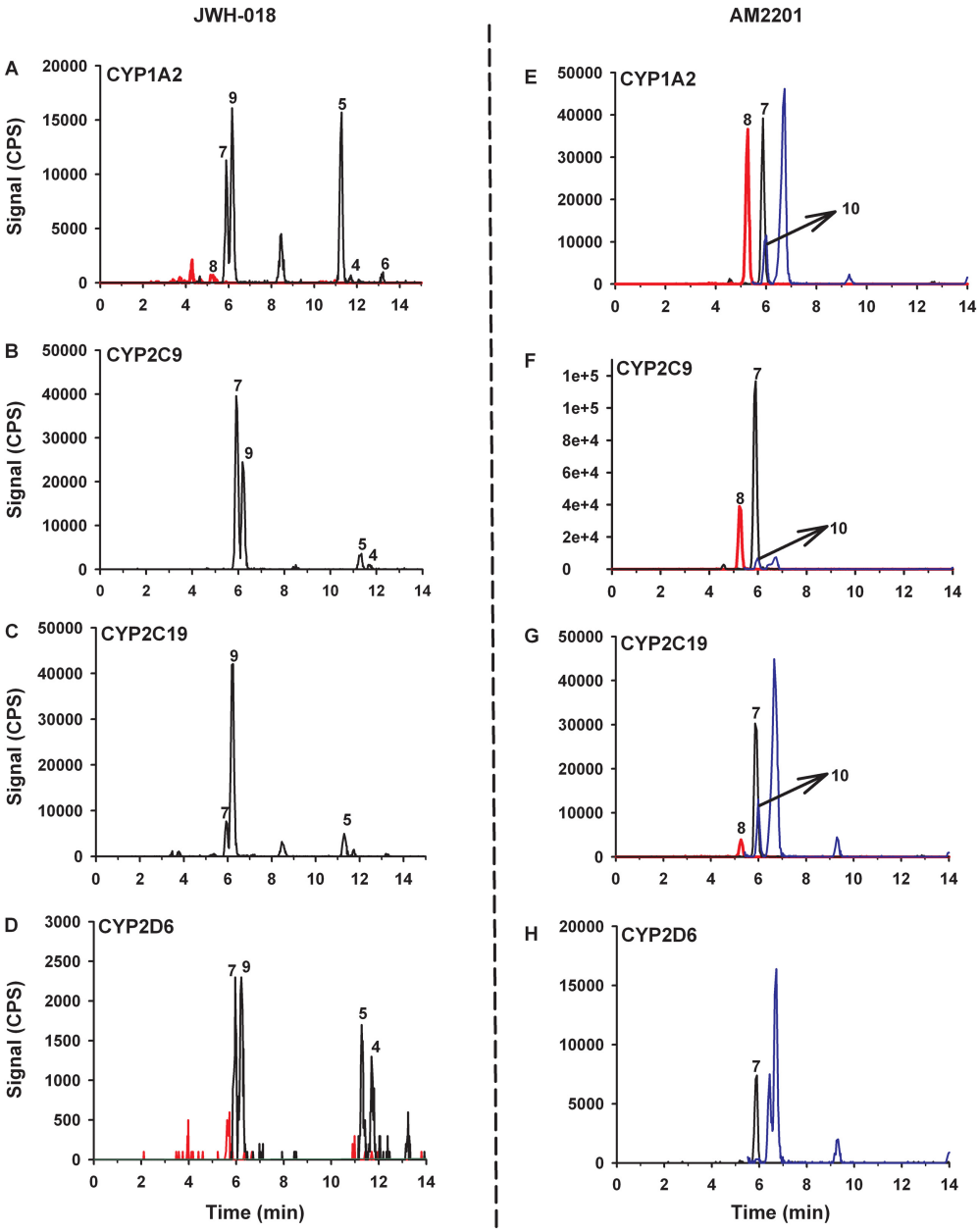

FIG. 4. LC chromatograms of the hydroxyl and carboxyl metabolites of JWH-018 and AM2201 produced from human cDNA-expressed recombinant P450s. Resulting chromatographs of hydroxylated and carboxylated metabolites produced from incubation of 10 μM JWH-018 with CYP1A2 (A), CYP2C9 (B), CYP2C19 (C), and CYP2D6 (D) and 10 μM AM2201 with CYP1A2 (E), CYP2C9 (F), CYP2C19 (G), and CYP2D6 (H) as mentioned under *Materials* and *Methods* are shown. The numbers above the chromatographic peaks correspond to the hydroxylated and carboxylated metabolites of JWH-018 and AM2201 shown in Fig. 1. Different color tracings are representative of the SRM experiments (Supplemental Table 1) used to detect analytes **1** to **10** (Fig. 1). Specific LC-MS/MS conditions are provided under *Materials and Methods*.

Fig. 3B). Formation of the ω-COOH metabolite common with JWH-018 and the distinct ω-1-OH metabolite of AM2201 followed Michaelis-Menten kinetics, whereas formation of the ω-OH metabolite exhibited a biphasic kinetic profile, consistent with microsomal enzyme preparations in which more than one type of enzyme is responsible for the formation of product.

Kinetic analysis of AM2201 oxidation with human recombinant CYP1A2 exhibited classic Michaelis-Menten kinetics for the formation ω-OH, ω-COOH, and ω-1-OH metabolites, with high affinity (low apparent K_m values ranging from 3.6–6.6 μM) and high capacity (V_{max} = 90–319 pmol of product · min^{-1} · nmol protein^{-1}). The ω-OH and ω-COOH metabolite formation with recombinant CYP2C9 exhibited Michaelis-Menten kinetics with high affinity (low apparent K_m = 2.4–7.2 μM) and high capacity (V_{max} = 266–309 pmol of product · min^{-1} · nmol protein^{-1}). However, the ω-1-OH metabolite formation with CYP2C9 followed substrate inhibition kinetics with high affinity (low apparent K_m = 7.2 μM) and high capacity (V_{max} = 122 pmol of product · min^{-1} · nmol protein^{-1}) (Table 2; Supplemental Fig. 5).

Although screening data indicate that the contribution of CYP2C19 and CYP2D6 in the hepatic metabolism of JWH-018 and AM2201 is minimal (Fig. 2), actual contributions can only be assessed through detailed kinetic evaluations. Largely, the kinetic profiles observed during either JWH-018 or AM2201 oxidation to form the ω-OH, ω-1-OH, and ω-COOH metabolites with recombinant CYP2C19 exhibited atypical kinetics. The reason for this is unknown and is a subject of further study. All K_m and V_{max} values reported in Table 1 are approximated. Concentrations of oxidized metabolites formed via CYP2D6 oxidation were low, but these reactions did exhibit classic Michaelis-Menten kinetics for the formation of ω-OH and ω-1-OH derivatives with high affinity (low apparent K_m = 2.8–3.2 μM) and low capacity (V_{max} = 26–43 pmol of product · min^{-1} · nmol protein^{-1}) when JWH-018 was used as the substrate (Table 1). When AM2201 was used, the same kinetic profiles were observed for each

TABLE 1

Kinetic parameters for JWH-018 oxidation

K_m and V_{max} values are given in micromolar concentrations and picomoles per minute per nanomole of protein for recombinant P450 isoforms and picomoles per minute per milligram of protein for HLM, respectively. V_{max} values represent the highest activity measured before inhibition is seen, and K_m values represent the lowest concentration of substrate that results in an activity of 1/2 "observed" V_{max}.

JWH-018 Metabolites	JWH-018 ω-OH	JWH-018 ω-COOH	JWH-018 ω-1-OH
CYP1A2			
V_{max}	833 ± 25	53 ± 9.4	1438 ± 32
K_m	5.3 ± 0.74	2.3 ± 0.80	4.7 ± 0.49
Kinetic fit	M-M	SI	M-M
CYP2C9			
V_{max}	835 ± 19	N.D.	487 ± 14
K_m	0.81 ± 0.07	N.D.	1.3 ± 0.13
Kinetic fit	Hill, n = 2.2	N.D.	Hill, n = 2.0
CYP2C19			
V_{max}	535	13,161	5157
K_m	82	36,648	106
Kinetic fit	—[a]	—	—
CYP2D6			
V_{max}	26 ± 1.0	N.D.	43 ± 2.0
K_m	2.8 ± 0.52	N.D.	3.2 ± 0.70
Kinetic fit	M-M	N.D.	M-M
HLM			
V_{max}	3.9 ± 0.25	N.D.	15.1 ± 1.5
K_m	7.8 ± 1.9	N.D.	26.3 ± 7.7
Kinetic fit	M-M	N.D.	M-M

M-M, Michaelis-Menten; SI, competitive substrate inhibition; N.D., not detected.
[a] —, the kinetic model did not fit the classic Hill equation for activation kinetics.

metabolite except for the ω-COOH metabolite. Formation of the ω-COOH metabolite exhibited atypical inhibition kinetics, which did not fit the classic competitive/uncompetitive-substrate inhibition models. K_m and V_{max} values presented in Table 2 are approximated.

To determine the major biotransformation pathways responsible for JWH-018 and AM2201 oxidation in human liver microsomes, intrinsic clearance (CL_{int}) (microlitres per minute per milligram of protein) was estimated for each metabolite. As shown in Table 3, more than 90% of JWH-018 is metabolized in human liver microsomes to form the 5-OH, 6-OH, ω-OH, and ω-1-OH metabolites. The intrinsic clearance of AM2201 follows a slightly different pathway, in which approximately 85% is metabolized to only the ω-OH and ω-COOH metabolites. The ω-1-OH and the unidentified-OH metabolites are formed to a much lesser extent.

To better assess the relative contribution of each cytochrome P450 isozyme, CL_{int} values (microliters per minute per nanomole of P450) for the formation of indole ring, alkyl side chain, and unidentified-OH metabolites of JWH-018 and AM2201 with recombinant CYP1A2, -2C9, -2C19, and -2D6 were calculated and normalized to hepatic abundance (Rowland-Yeo et al., 2003; Proctor et al., 2004). The metabolic fraction ($f_{m,CYP}$) calculations presented in Table 4 identify CYP2C9 as the primary isozyme responsible for the metabolism of JWH-018 to its ω-OH and ω-1-OH derivatives ($f_{m,2C9}$ = ~0.83–0.90 and 0.48–0.62, respectively); whereas CYP1A2 appears to be responsible for ω-COOH formation ($f_{m,1A2}$ = 1). CYP2C9 and CYP1A2 also appear to play an important role in oxidizing AM2201 to the corresponding ω-OH, ω-1-OH, and ω-COOH metabolites with $f_{m,2C9}$ ranging from 0.48 to 0.76 and $f_{m,1A2}$ ranging from 0.11 to 0.49 (Table 5). Both CYP1A2 and CYP2C9 also appear to catalyze the formation of the unidentified-OH metabolite of AM2201 ($f_{m,1A2}$ = ~0.42–0.56 and $f_{m,2C9}$ = ~0.29–0.40), but the physiological significance of this metabolite remains to be determined. CYP2C19 and CYP2D6 contributions to JWH-018 and AM2201 hepatic oxidation seem to be negligible (Tables 4 and 5). However, CYP2C19 catalyzed some formation of the unidentified-OH metabolite of AM2201 ($f_{m,2C19}$ = 0.19) (Supplemental Table 5).

Pharmacological/Toxicological Evaluations: CB_1 Receptor Binding and Intrinsic Activity. To begin understanding the pharmacological and/or toxicological consequences of synthetic cannabinoid metabolism, we used CB_1 receptor binding and intrinsic activity assays to determine whether cytochrome P450-mediated biotransformation led to the formation of biologically active intermediates or whether oxidation terminated activity at the cannabinoid receptor. We have previously reported the binding affinity for several of the indole ring-oxidized metabolites and the fact that the ω-COOH metabolite of JWH-018 does not bind to the CB_1 receptor (Brents et al., 2011). However, the primary metabolites, with the exception of ω-OH derivative, have never been investigated for CB_1 receptor binding and intrinsic activity assays. Studies presented here are similar to our previous report (Brents et al., 2011). In addition, these studies showed that JWH-018, AM2201, and their ω-OH and ω-1-OH metabolites, but not the ω-COOH metabolite, bind to the CB_1 receptor with high affinity. JWH-018, AM2201, and its ω-OH and ω-1-OH metabolites showed high affinity (K_i = ~0.4–35 nM), resulting in complete displacement of [^{3}H]CP-55,940 from the CB_1 receptor (Fig. 5, A and B). The relative rank order of binding affinity for all the compounds tested was AM2201 = JWH-018 > JWH-018/AM2201 ω-1-OH = JWH-018 ω-OH. More importantly, the CB_1 receptor affinity was higher for JWH-018 and AM2201, and similar for ω-OH and ω-1-OH derivatives of each synthetic cannabinoid (Fig. 5) compared with the affinity of Δ^9-THC (15.3 nM) for CB_1 receptors (Brents et al., 2011).

The ability of JWH-018, AM2201, and ω-OH, ω-1-OH, and ω-COOH metabolites to activate G-proteins after binding to the CB_1 receptors was investigated using the [^{35}S]GTPγS binding assay (Fig. 6A). A receptor saturating concentration (10 μM) of CP-55,940, Δ^9-THC, JWH-018, AM2201, and their ω-OH, ω-1-OH, and ω-COOH derivatives was used to determine a measure of maximal efficacy produced by activation of CB_1 receptors in mouse brain membranes. CP-55,940, JWH-018, AM2201, and JWH-018 ω-OH and ω-1-OH and AM2201 ω-1-OH metabolites produced a similar

TABLE 2

Kinetic parameters for AM2201 oxidation

K_m and V_{max} values are given in micromolar concentrations and picomoles per minute per nanomole of protein for recombinant P450 isoforms and picomoles per minute per milligram of protein for HLM, respectively.

AM2201 Metabolites	JWH-018 ω-OH	JWH-018 ω-COOH	AM2201 ω-1-OH
CYP1A2			
V_{max}	90 ± 5.2	319 ± 12	154 ± 7.3
K_m	4.8 ± 1.2	3.6 ± 0.64	6.6 ± 1.3
Kinetic fit	M-M	M-M	M-M
CYP2C9			
V_{max}	309 ± 12	266 ± 12	122 ± 28
K_m	4.9 ± 0.80	2.4 ± 0.52	7.2 ± 3.2
Kinetic fit	M-M	M-M	SI
CYP2C19			
V_{max}	202 ± 2.9	44 ± 1.5	315
K_m	6.3 ± 2.1	1.6 ± 0.30	334
Kinetic fit	SI	M-M	Hill, n = 0.4[a]
CYP2D6			
V_{max}	24 ± 1.4	8.9	N.D.
K_m	6.5 ± 1.6	24	N.D.
Kinetic fit	M-M	—[b]	N.D.
HLM			
V_{max}	2.8 ± 0.3	3.3 ± 0.16	0.92 ± 0.07
K_m	5.8 ± 1.3	5.5 ± 1.2	7.4 ± 2.1
Kinetic fit	Biphasic	M-M	M-M

M-M, Michaelis-Menten; SI, competitive substrate inhibition; N.D., not detected.
[a]Kinetic model did not fit classic Hill equation for activation kinetics.
[b]Kinetic model did not fit the classic competitive/uncompetitive-substrate inhibition models.

TABLE 3

CL_{int} and relative percent calculations for each metabolite of JWH-018 and AM2201 produced in pooled HLM

Intrinsic clearance values are given in microliters per minute per milligram of protein.

Substrate	Minor Metabolites				Major Metabolites			Total
	5-OH	6-OH	7-OH	Unidentified-OH	ω-OH	ω-COOH	ω-1-OH	
JWH-018								
CL_{int}	0.520	1.0	0	0.18	0.5	0	0.574	2.77
%	19	36	0	6.4	18	0	21	100
AM2201								
CL_{int}	0	0	0	0.102	0.483	0.60	0.124	1.31
%	0	0	0	7.8	37	46	9.5	100

level of G-protein activation (Fig. 6A), and in this assay appear to act as full CB_1 receptor agonists, similar to CP-55,940. The intrinsic efficacy (G-protein activation) of JWH-018, AM2201, and their ω-OH and ω-1-OH metabolites was statistically greater ($p < 0.05$) than that of the partial agonist and principal psychoactive ingredient of marijuana, Δ^9-THC (Fig. 6A). As might be expected on the basis of poor CB_1 receptor affinity, the ω-COOH derivative of JWH-018 did not stimulate G-proteins (Fig. 6A). Coincubation with a receptor saturating concentration (1 μM) of the CB_1 receptor antagonist O-2050 significantly attenuated G-protein activation elicited by all compounds examined, strongly suggesting CB_1 receptor selectivity of these compounds (Fig. 6B). Of importance, O-2050 demonstrated no significant effects on basal G-protein activity when administered alone (data not shown). The CB_1 receptor activation elicited by ω-OH and ω-1-OH metabolites indicates that cytochrome P450-mediated oxidation of JWH-018 and AM2201 leads to the formation of potent and efficacious metabolites that retain significant affinity and activity at CB_1 receptors.

Discussion

In 2005, synthetic cannabinoid products, marketed as K2/Spice emerged as new drugs of abuse and have been gaining popularity worldwide ever since. Today, there are significant public health concerns related to these psychoactive drugs of abuse with one in nine high school students admitting use of K2 (Hu et al., 2011). Furthermore, there is increasing morbidity and mortality reports related to these potent human cannabinoid receptor agonists, which were originally synthesized to study CB_1 and CB_2 receptors and their potential antiemetic and pain-relieving therapeutic properties. There is an urgent need to elucidate the pharmacology of these substances in humans. Before pharmacokinetic and pharmacodynamic properties can be adequately studied in humans, metabolic pathways leading to metabolism and elimination and pathways leading to the generation of biologically active metabolites must be delineated. Therefore, the purpose of the present study was to identify specific P450 isoforms responsible for JWH-018 and AM2201 metabolism and to compare the relative affinity and intrinsic activity of the primary human metabolites at CB_1 receptors.

After the discovery of Δ^9-THC as the primary psychoactive constituent of cannabis, several studies (Wall et al., 1983; Bornheim et al., 1992; Watanabe et al., 1995, 2007; Bland et al., 2005) demonstrated that Δ^9-THC is primarily metabolized to a single active metabolite, 11-OH-Δ^9-THC, by CYP2C9 and to various inactive oxidized products by CYP3A4. In contrast, this study identifies CYP2C9 and CYP1A2 as primary P450 isoforms involved in the oxidation of the psychoactive synthetic cannabinoids JWH-018 and AM2201. In vitro HLM incubation of JWH-018 and AM2201 primarily led to the formation of alkyl side chain-oxidized metabolites that the mirrored metabolic patterns observed in human urine specimens collected after suspected JWH-018 or AM2201 use. Indole ring-oxidized metabolites and two unidentified hydroxylated metabolites were also produced in vitro, but the physiological significance of these findings remains to be determined. Consistent with data presented in this report, studies have

TABLE 4

Fractional contribution of rP450 isoforms during JWH-018 oxidation

CL_{int} values are given in microliters per minute per nanomole of P450 and hepatic abundance values of specific P450s (Rowland-Yeo et al., 2003; Proctor et al., 2004) are given in nanomoles per milligram of protein.

JWH-018 Metabolites	CL_{int} in rP450	Hepatic Abundance	Fractional Contribution of Each P450 ($f_{m,CYP}$)
CYP1A2			
ω-OH	157		0.066–0.097
ω-COOH	23	0.045–0.052	1.0
ω-1-OH	306		0.27–0.36
CYP2C9			
ω-OH	1035		0.83–0.90
ω-COOH	0	0.032–0.073	0
ω-1-OH	375		0.48–0.62
CYP2C19			
ω-OH	6.5		0.001–0.002
ω-COOH	0	0.006–0.014	0
ω-1-OH	48.7		0.0011–0.0018
CYP2D6			
ω-OH	9.3		0.001–0.002
ω-COOH	0	0.009–0.01	0
ω-1-OH	13.4		0.003–0.005

rP450, recombinant human cytochrome P450.

TABLE 5

Fractional contribution of recombinant human P450 isoforms during AM2201 oxidation

CL_{int} values are given in microliters per minute per nanomole of P450 and hepatic abundance values of specific P450s (Rowland-Yeo et al., 2003; Proctor et al., 2004) are given in nanomoles per milligram of protein.

AM2201 Metabolites	CL_{int} in rP450	Hepatic Abundance	Fractional Contribution of Each P450 ($f_{m,CYP}$)
CYP1A2			
ω-OH	19		0.11–0.16
ω-COOH	89	0.045–0.052	0.26–0.35
ω-1-OH	23		0.39–0.49
CYP2C9			
ω-OH	63		0.67–0.76
ω-COOH	111	0.032–0.073	0.48–0.70
ω-1-OH	17		0.36–0.52
CYP2C19			
ω-OH	32		0.059–0.091
ω-COOH	28	0.006–0.014	0.021–0.030
ω-1-OH	0.940		0.003–0.010
CYP2D6			
ω-OH	3.7		0.001–0.005
ω-COOH	0.371	0.009–0.01	0.0005–0.002
ω-1-OH	0		0

rP450, recombinant human cytochrome P450.

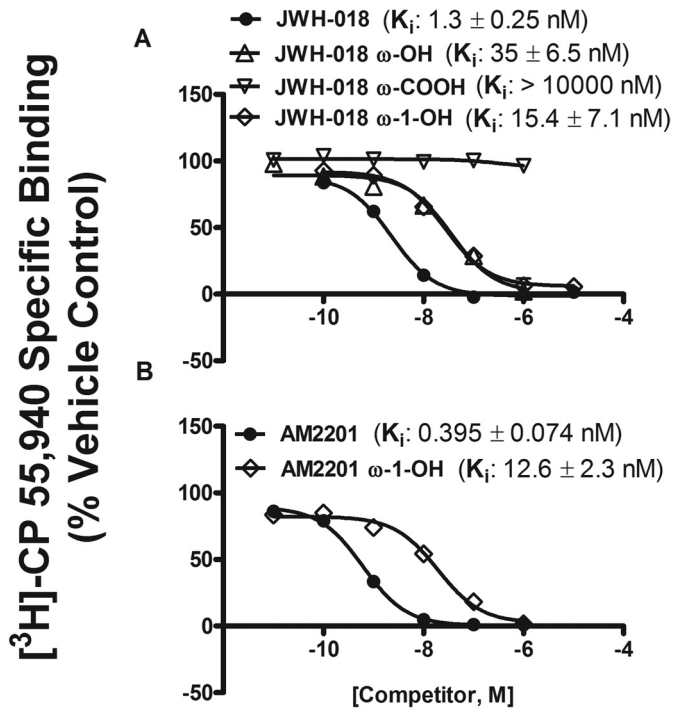

FIG. 5. JWH-018 and its ω-OH and ω-1-OH metabolites (A) and AM2201 and its ω-1-OH metabolite (B) bind the CB_1 receptor with nanomolar affinity. JWH-018, AM2201, and ω-OH and ω-1-OH metabolites, but not the ω-COOH metabolite, completely displaced the radiolabeled cannabinoid [^{3}H]CP-55,940 from the CB_1 receptor.

consistently identified the alkyl side chain-oxidized metabolites as the primary circulating and thus potentially bioavailable derivatives (Kacinko et al., 2011). Human studies have also demonstrated that glucuronic acid conjugation is required for urinary excretion (Chimalakonda et al., 2011b; Moran et al., 2011) of synthetic cannabinoids.

The present study identified CYP2C9 and CYP1A2 as the primary enzymes involved in the hepatic oxidation of JWH-018 and AM2201. CYP2C9 is one of the major human polymorphic enzymes, with the most common allelic variants showing reduced rates of metabolism toward substrates (Ortiz de Montellano, 1995). This enzyme is highly expressed both in the liver and intestine (Paine et al., 2006) and is involved in the metabolism of Δ^9-THC and approximately 16% of drugs in current clinical use, such as fluoxetine, escitalopram, citalopram, lithium, valproic acid, aripiprazole, and risperidone (Ortiz de Montellano, 1995). Given the high abundance of CYP2C9 in the intestine, it is anticipated that this isoform will be intricately involved in the intestinal metabolism of synthetic cannabinoids taken orally, as well as other routes of exposures. Consideration of oral routes of exposure is important because we have previously shown that ingestion of JWH-018 can lead to rapid and severe toxicity in humans (Lapoint et al., 2011). Toxic drug-drug interactions are also an important concern for public health officials, especially because hepatic intrinsic clearance associated with CYP2C9 metabolism is greater than 50%. CYP1A2 also contributed significantly to the hepatic metabolism of JWH-018 and AM2201. This isozyme is involved in the biotransformation of 5 to 10% of drugs in current clinical use and is known to be differentially expressed in humans, suggesting polymorphic control of enzyme activity (Ortiz de Montellano, 1995). Therefore, individuals with significantly lower expression of CYP1A2 would be predicted to have a decreased capacity for synthetic cannabinoid detoxification and may be at increased risks for adverse consequences.

Although the involvement of CYP2C19 and CYP2D6 in the overall hepatic metabolism of JWH-018 and AM2201 is minimal, the physiological importance of these enzymes in other tissues remains to be

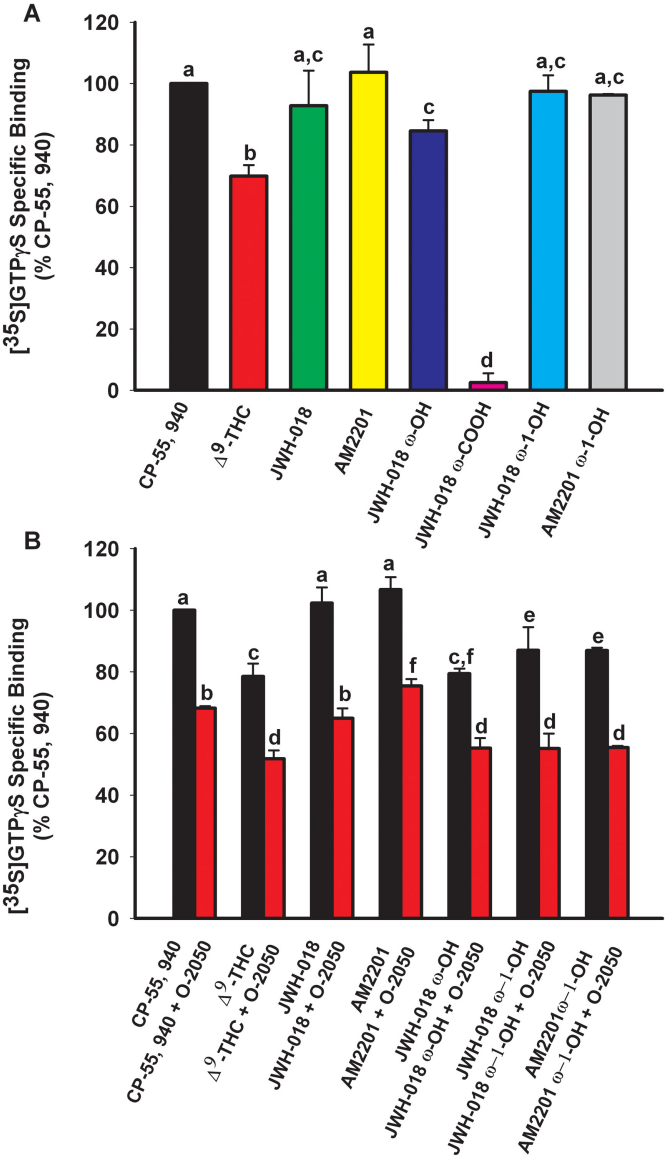

FIG. 6. A, JWH-018, AM2201, and their ω-OH and ω-1-OH metabolites activate mouse CB_1 receptor; 10 μM JWH-018 and its ω-OH and ω-1-OH metabolites activated mouse CB_1 receptor with greater efficacy than 10 μM Δ^9-THC. JWH-018, AM2201, and the ω-1-OH metabolites of each displayed full agonist activity comparable to that of CP-55,940. The ω-OH metabolite of JWH-018 displayed efficacy similar to that of the parent drug. No G-protein activity was observed with the ω-COOH metabolite of JWH-018. [^{35}S]GTPγS specific binding is expressed as a percentage of CP-55,940 specific binding. Values designated with different letters above the error bars are significantly different ($p < 0.05$, one-way ANOVA with Newman-Keuls multiple comparison post hoc test, $n = 3$). B, G-protein stimulation in mouse brain by JWH-018, AM2201, and their ω-OH and ω-1-OH metabolites is blocked by CB_1 receptor selective neutral antagonist O-2050. G-protein activation by 1 μM CP-55,940 and JWH-018 is blocked to a similar extent by 1 μM O-2050. Significant attenuation of G-protein stimulation by 1 μM AM2201 is blocked by 1 μM O-2050. G-protein stimulation by 1 μM Δ^9-THC, ω-OH, and ω-1-OH metabolites of JWH-018 and AM2201 is blocked to a similar extent by 1 μM O-2050. [^{35}S]GTPγS specific binding is expressed as a percentage of CP-55,940. Values designated with different letters above the error bars are significantly different ($p < 0.05$, one-way ANOVA with Newman-Keuls multiple comparison post hoc test, $n = 3$).

determined. For example, it is well established that CYP2D6 is involved in the metabolism of many central nervous system-acting drugs (Ingelman-Sundberg, 2005) and that this P450 is one of the major mixed-function oxidases highly expressed in cerebral cortex, hippocampus, and cerebellum, regions known for high expression of CB_1 receptors (Meyer et al., 2007). CYP2D6 is highly polymorphic, with more than 80 variant alleles identified to date, including the nonfunctional *CYP2D6*4* null allele, present in 12 to 21% of whites (Ingelman-Sundberg, 2005). Of importance, CYP2D6 is known to metabolize the endocannabinoid anandamide (Snider et al., 2008), which suggests that this enzyme may also interact with other synthetic cannabinoids like JWH-018 and AM2201 in the brain. Although speculative, data presented in this report suggest that CYP2D6 may be critical in controlling brain concentrations of parent synthetic cannabinoids and their active metabolites.

Another critical finding presented in this study is that JWH-018, AM2201, and their major hydroxylated metabolites produced in vitro and in humans exposed to these synthetic cannabinoids bind to and activate CB_1 receptors with nanomolar affinity. These data are in stark contrast to binding data for Δ^9-THC. All Δ^9-THC metabolites, except 11-OH-Δ^9-THC, are inactivated by oxidative metabolism, which prevents further CB_1 receptor activation (Adams and Martin, 1996). The higher affinity, potency, and efficacy of JWH-018 and AM2201, coupled with its potential metabolism to a number of equally active metabolites, suggests that both acute and chronic effects of K2 may be intensified compared with a similar level of exposure to marijuana. In relation to Δ^9-THC, the results presented herein suggest that differences in synthetic cannabinoid metabolism may lead to differential pharmacokinetic and pharmacodynamic properties and might offer explanations for the widely observed adverse clinical manifestations of synthetic cannabinoid abuse.

Data from the present study provide critical missing information related to the metabolism and toxicological properties of K2 parent compounds and their human metabolites, including mechanism(s) of action at cannabinoid receptor subtypes. The findings of the present study provide the groundwork for studying potential mechanisms of toxicity in humans and establish a basis for developing widely available screening tools for detecting K2 abuse. Of importance, data demonstrate that the synthetic cannabinoid compounds have a greater toxicity potential in comparison with Δ^9-THC because of their unique metabolic profiles and drug/metabolite binding characteristics, which may predispose humans to a constellation of serious adverse effects reported after K2 use.

Authorship Contributions

Participated in research design: Chimalakonda, Brents, C. L. Moran, James, Hollenberg, Prather, Radominska-Pandya, and J. H. Moran.

Conducted experiments: Chimalakonda.

Performed data analysis: Chimalakonda, Bratton, Brents, Radominska-Pandya, and J. H. Moran.

Wrote or contributed to the writing of the manuscript: Chimalakonda, Seely, Bratton, Brents, C. L. Moran, Endres, James, Hollenberg, Prather, Radominska-Pandya, and J. H. Moran.

References

Adams IB and Martin BR (1996) Cannabis: pharmacology and toxicology in animals and humans. *Addiction* **91:**1585–1614.

Atwood BK, Huffman J, Straiker A, and Mackie K (2010) JWH018, a common constituent of 'Spice' herbal blends, is a potent and efficacious cannabinoid CB receptor agonist. *Br J Pharmacol* **160:**585–593.

Banken JA (2004) Drug abuse trends among youth in the United States. *Ann NY Acad Sci* **1025:**465–471.

Benford DM and Caplan JP (2011) Psychiatric sequelae of Spice, K2, and synthetic cannabinoid receptor agonists. *Psychosomatics* **52:**295.

Bland TM, Haining RL, Tracy TS, and Callery PS (2005) CYP2C-catalyzed Δ^9-tetrahydrocannabinol metabolism: kinetics, pharmacogenetics and interaction with phenytoin. *Biochem Pharmacol* **70:**1096–1103.

Bornheim LM, Lasker JM, and Raucy JL (1992) Human hepatic microsomal metabolism of Δ^1-tetrahydrocannabinol. *Drug Metab Dispos* **20:**241–246.

Brents LK, Gallus-Zawada A, Radominska-Pandya A, Vasiljevik T, Prisinzano TE, Fantegrossi WE, Moran JH, and Prather PL (2012) Monohydroxylated metabolites of the K2 synthetic cannabinoid JWH-073 retain intermediate to high cannabinoid 1 receptor (CB1R) affinity and exhibit neutral antagonist to partial agonist activity. *Biochem Pharmacol* **83:**952–961.

Brents LK, Reichard EE, Zimmerman SM, Moran JH, Fantegrossi WE, and Prather PL (2011) Phase I hydroxylated metabolites of the K2 synthetic cannabinoid JWH-018 retain in vitro and in vivo cannabinoid 1 receptor affinity and activity. *PLoS One* **6:**e21917.

Budney AJ and Hughes JR (2006) The cannabis withdrawal syndrome. *Curr Opin Psychiatry* **19:**233–238.

Camp NE (2011) Synthetic cannabinoids. *J Emerg Nurs* **37:**292–293.

Cheng Y and Prusoff WH (1973) Relationship between the inhibition constant (K1) and the concentration of inhibitor which causes 50 per cent inhibition (I50) of an enzymatic reaction. *Biochem Pharmacol* **22:**3099–3108.

Chimalakonda KC, Bratton SM, Le VH, Yiew KH, Dineva A, Moran CL, James LP, Moran JH, and Radominska-Pandya A (2011a) Conjugation of synthetic cannabinoids JWH-018 and JWH-073, metabolites by human UDP-glucuronosyltransferases. *Drug Metab Dispos* **39:** 1967–1976.

Chimalakonda KC, Moran CL, Kennedy PD, Endres GW, Uzieblo A, Dobrowolski PJ, Fifer EK, Lapoint J, Nelson LS, Hoffman RS, et al. (2011b) Solid-phase extraction and quantitative measurement of omega and omega-1 metabolites of JWH-018 and JWH-073 in human urine. *Anal Chem* **83:**6381–6388.

Compton DR, Gold LH, Ward SJ, Balster RL, and Martin BR (1992a) Aminoalkylindole analogs: cannabimimetic activity of a class of compounds structurally distinct from Δ^9-tetrahydrocannabinol. *J Pharmacol Exp Ther* **263:**1118–1126.

Compton DR, Johnson MR, Melvin LS, and Martin BR (1992b) Pharmacological profile of a series of bicyclic cannabinoid analogs: classification as cannabimimetic agents. *J Pharmacol Exp Ther* **260:**201–209.

Dresen S, Ferreirós N, Pütz M, Westphal F, Zimmermann R, and Auwärter V (2010) Monitoring of herbal mixtures potentially containing synthetic cannabinoids as psychoactive compounds. *J Mass Spectrom* **45:**1186–1194.

European Monitoring Centre for Drugs and Drug Addiction (2009) Understanding the 'Spice' phenomenon, in *EMCDDA 2009*, pp 1–25, Office for Official Publications of the European Communities, Lisbon, Portugal.

Every-Palmer S (2011) Synthetic cannabinoid JWH-018 and psychosis: an explorative study. *Drug Alcohol Depend* **117:**152–157.

Hu X, Primack BA, Barnett TE, and Cook RL (2011) College students and use of K2: an emerging drug of abuse in young persons. *Subst Abuse Treat Prev Policy* **6:**16.

Huffman JW and Padgett LW (2005) Recent developments in the medicinal chemistry of cannabimimetic indoles, pyrroles and indenes. *Curr Med Chem* **12:**1395–1411.

Hutter M, Broecker S, Kneisel S, and Auwärter V (2012) Identification of the major urinary metabolites in man of seven synthetic cannabinoids of the aminoalkylindole type present as adulterants in 'herbal mixtures' using LC-MS/MS techniques. *J Mass Spectrom* **47:**54–65.

Ingelman-Sundberg M (2005) Genetic polymorphisms of cytochrome P450 2D6 (CYP2D6): clinical consequences, evolutionary aspects and functional diversity. *Pharmacogenomics J* **5:**6–13.

Jones RT (2002) Cardiovascular system effects of marijuana. *J Clin Pharmacol* **42:**58S–63S.

Kacinko SL, Xu A, Homan JW, McMullin MM, Warrington DM, and Logan BK (2011) Development and validation of a liquid chromatography-tandem mass spectrometry method for the identification and quantification of JWH-018, JWH-073, JWH-019, and JWH-250 in human whole blood. *J Anal Toxicol* **35:**386–393.

Kudo K, Nagata T, Kimura K, Imamura T, and Jitsufuchi N (1995) Sensitive determination of Δ^9-tetrahydrocannabinol in human tissues by GC-MS. *J Anal Toxicol* **19:**87–90.

Lapoint J, James LP, Moran CL, Nelson LS, Hoffman RS, and Moran JH (2011) Severe toxicity following synthetic cannabinoid ingestion. *Clin Toxicol (Phila)* **49:**760–764.

Mackie K (2008) Cannabinoid receptors: where they are and what they do. *J Neuroendocrinol* **20 (Suppl 1):**10–14.

Meyer RP, Gehlhaus M, Knoth R, and Volk B (2007) Expression and function of cytochrome p450 in brain drug metabolism. *Curr Drug Metab* **8:**297–306.

Moran CL, Le VH, Chimalakonda KC, Smedley AL, Lackey FD, Owen SN, Kennedy PD, Endres GW, Ciske FL, Kramer JB, et al. (2011) Quantitative measurement of JWH-018 and JWH-073 metabolites excreted in human urine. *Anal Chem* **83:**4228–4236.

Müller H, Sperling W, Köhrmann M, Huttner HB, Kornhuber J, and Maler JM (2010) The synthetic cannabinoid Spice as a trigger for an acute exacerbation of cannabis induced recurrent psychotic episodes. *Schizophr Res* **118:**309–310.

Ortiz de Montellano PR (1995) Human Cytochrome P450 enzymes, in *Cytochrome P-450: Structure, Mechanism, and Biochemistry*, 2nd ed., (Ortiz De Montellano PR ed), pp 473–535, Plenum Publishing Corp, New York.

Paine MF, Hart HL, Ludington SS, Haining RL, Rettie AE, and Zeldin DC (2006) The human intestinal cytochrome P450 "pie." *Drug Metab Dispos* **34:**880–886.

Pant S, Deshmukh A, Dholaria B, Kaur V, Ramavaram S, Ukor M, and Teran GA (2012) Spicy seizure. *Am J Med Sci* **344:**67–68.

Prather PL, Martin NA, Breivogel CS, and Childers SR (2000) Activation of cannabinoid receptors in rat brain by WIN 55212-2 produces coupling to multiple G protein α-subunits with different potencies. *Mol Pharmacol* **57:**1000–1010.

Proctor NJ, Tucker GT, and Rostami-Hodjegan A (2004) Predicting drug clearance from recombinantly expressed CYPs: intersystem extrapolation factors. *Xenobiotica* **34:**151–178.

Randall MD, Kendall DA, and O'Sullivan S (2004) The complexities of the cardiovascular actions of cannabinoids. *Br J Pharmacol* **142:**20–26.

Rowland-Yeo K, Rostami-Hodjegan A, and Tucker GT (2003) Abundance of cytochrome P450 in human liver: a meta-analysis, in *Proceedings of the British Pharmacology Society Winter Meeting*; 2003 Dec 16–18; London, UK. British Pharmacology Society, London, UK.

Schneir AB, Cullen J, and Ly BT (2011) "Spice" girls: synthetic cannabinoid intoxication. *J Emerg Med* **40:**296–299.

Seely KA, Lapoint J, Moran JH, and Fattore L (2012) Spice drugs are more than harmless herbal blends: a review of the pharmacology and toxicology of synthetic cannabinoids. *Prog Neuropsychopharmacol Biol Psychiatry* http://dx.doi.org/10.1016/j.pnpbp.2012.04.017.

Seely KA, Prather PL, James LP, and Moran JH (2011) Marijuana-based drugs: innovative therapeutics or designer drugs of abuse? *Mol Interv* **11:**36–51.

Shoemaker JL, Joseph BK, Ruckle MB, Mayeux PR, and Prather PL (2005) The endocannabinoid noladin ether acts as a full agonist at human CB2 cannabinoid receptors. *J Pharmacol Exp Ther* **314:**868–875.

Simmons J, Cookman L, Kang C, and Skinner C (2011a) Three cases of "spice" exposure. *Clin Toxicol (Phila)* **49:**431–433.

Simmons JR, Skinner CG, Williams J, Kang CS, Schwartz MD, and Wills BK (2011b) Intoxication from smoking "spice." *Ann Emerg Med* **57:**187–188.

Snider NT, Sikora MJ, Sridar C, Feuerstein TJ, Rae JM, and Hollenberg PF (2008) The endocannabinoid anandamide is a substrate for the human polymorphic cytochrome P450 2D6. *J Pharmacol Exp Ther* **327:**538–545.

Sobolevsky T, Prasolov I, and Rodchenkov G (2010) Detection of JWH-018 metabolites in smoking mixture post-administration urine. *Forensic Sci Int* **200:**141–147.

Thakur GA, Nikas SP, and Makriyannis A (2005) CB1 cannabinoid receptor ligands. *Mini Rev Med Chem* **5:**631–640.

Vearrier D and Osterhoudt KC (2010) A teenager with agitation: higher than she should have climbed. *Pediatr Emerg Care* **26:**462–465.

Wall ME, Sadler BM, Brine D, Taylor H, and Perez-Reyes M (1983) Metabolism, disposition, and kinetics of Δ^9-tetrahydrocannabinol in men and women. *Clin Pharmacol Ther* **34:**352–363.

Ward SJ, Baizman E, Bell M, Childers S, D'Ambra T, Eissenstat M, Estep K, Haycock D, Howlett A, and Luttinger D (1990) Aminoalkylindoles (AAIs): a new route to the cannabinoid receptor? *NIDA Res Monogr* **105:**425–426.

Watanabe K, Matsunaga T, Yamamoto I, Funae Y, and Yoshimura H (1995) Involvement of CYP2C in the metabolism of cannabinoids by human hepatic microsomes from an old woman. *Biol Pharm Bull* **18:**1138–1141.

Watanabe K, Yamaori S, Funahashi T, Kimura T, and Yamamoto I (2007) Cytochrome P450 enzymes involved in the metabolism of tetrahydrocannabinols and cannabinol by human hepatic microsomes. *Life Sci* **80:**1415–1419.

Wells DL and Ott CA (2011) The "new" marijuana. *Ann Pharmacother* **45:**414–417.

Wintermeyer A, Möller I, Thevis M, Jübner M, Beike J, Rothschild MA, and Bender K (2010) In vitro phase I metabolism of the synthetic cannabimimetic JWH-018. *Anal Bioanal Chem* **398:**2141–2153.

Young AC, Schwarz E, Medina G, Obafemi A, Feng SY, Kane C, and Kleinschmidt K (2011) Cardiotoxicity associated with the synthetic cannabinoid, K9, with laboratory confirmation. *Am J Emerg Med* **30:**1320.e5–1320.e7.

Zhang Q, Ma P, Iszard M, Cole RB, Wang W, and Wang G (2002) In vitro metabolism of *R*(+)-[2,3-dihydro-5-methyl-3-[(morpholinyl)methyl]pyrrolo [1,2,3-de]1,4-benzoxazinyl]-(1-naphthalenyl) methanone mesylate, a cannabinoid receptor agonist. *Drug Metab Dispos* **30:**1077–1086.

Zimmermann US, Winkelmann PR, Pilhatsch M, Nees JA, Spanagel R, and Schulz K (2009) Withdrawal phenomena and dependence syndrome after the consumption of "spice gold." *Dtsch Arztebl Int* **106:**464–467.

Address correspondence to: Dr. Jeffery H. Moran, Arkansas Department of Health, Public Health Laboratory, 201 S. Monroe St., Little Rock, AR 72205. E-mail: jeffery.moran@arkansas.gov